

LETTERS

A central integrator of transcription networks in plant stress and energy signalling

Elena Baena-González^{1*}, Filip Rolland^{1,2,3*}, Johan M. Thevelein^{2,3} & Jen Sheen¹

Photosynthetic plants are the principal solar energy converter sustaining life on Earth. Despite its fundamental importance, little is known about how plants sense and adapt to darkness in the daily light–dark cycle, or how they adapt to unpredictable environmental stresses that compromise photosynthesis and respiration and deplete energy supplies. Current models emphasize diverse stress perception and signalling mechanisms^{1,2}. Using a combination of cellular and systems screens, we show here that the evolutionarily conserved *Arabidopsis thaliana* protein kinases, KIN10 and KIN11 (also known as AKIN10/At3g01090 and AKIN11/At3g29160, respectively), control convergent reprogramming of transcription in response to seemingly unrelated darkness, sugar and stress conditions. Sensing and signalling deprivation of sugar and energy, KIN10 targets a remarkably broad array of genes that orchestrate transcription networks, promote catabolism and suppress anabolism. Specific bZIP transcription factors partially mediate primary KIN10 signalling. Transgenic KIN10 overexpression confers enhanced starvation tolerance and lifespan extension, and alters architecture and developmental transitions. Significantly, double *kin10 kin11* deficiency abrogates the transcriptional switch in darkness and stress signalling, and impairs starch mobilization at night and growth. These studies uncover surprisingly pivotal roles of KIN10/11 in linking stress, sugar and developmental signals to globally regulate plant metabolism, energy balance, growth and survival. In contrast to the prevailing view that sucrose activates plant SnRK1s (Snf1-related protein kinases)^{3–6}, our functional analyses of *Arabidopsis* KIN10/11 provide compelling evidence that SnRK1s are inactivated by sugars and share central roles with the orthologous yeast Snf1 and mammalian AMPK in energy signalling.

We surveyed the public transcriptome databases using the genome tool Genevestigator⁷ and discovered that dark-induced (*DIN*) genes are activated under diverse stress conditions and repressed by sugars and light (Supplementary Fig. 2a). Consistently, quantitative analyses confirmed that *DIN1* (At4g35770) and *DIN6* (At3g47340) were activated by various stresses—such as darkness, herbicide (3-(3,4-dichlorophenyl)-1,1-dimethylurea, DCMU)⁸ and flooding/submergence—that limit photosynthesis and respiration, and hence sugar and energy supplies in isolated mesophyll cells and whole plants. This activation was antagonized by both glucose and sucrose (Fig. 1a–c, and Supplementary Fig. 2b). The results suggest that plant cells sense sugar or energy depletion in a cell-autonomous manner and trigger convergent gene activation in response to diverse and seemingly unrelated stress signals independent of light.

We have previously shown that the *Arabidopsis* glucose sensor hexokinase 1 (HXK1) is essential for the glucose repression of photosynthesis genes⁹. However, *DIN* gene repression by glucose in

the dark was still active in the *HXK1*-null mutant *gin2* (*glucose-insensitive2*) (Fig. 1c), indicating the involvement of an HXK1-independent signalling pathway¹⁰. To identify the key regulators governing this stress/sugar signalling pathway, we developed a cell

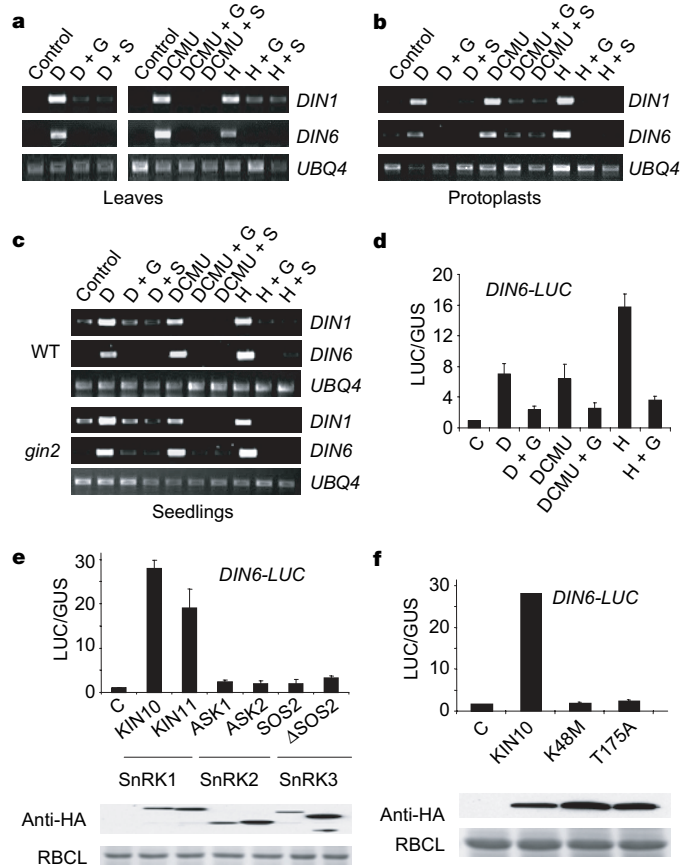


Figure 1 | *DIN* genes are activated by diverse stresses and repressed by sugars. Stress induces *DIN* gene expression in *Arabidopsis* leaves (a), and isolated mesophyll cells (b). The induction is diminished by glucose (G) and sucrose (S). c, The *gin2* mutant exhibits normal *DIN* gene induction and sugar repression. d, Diverse stresses activate the *DIN6-LUC* reporter. Glucose antagonizes *DIN6-LUC* activation. e, *DIN6-LUC* is specifically activated by SnRK1s. f, *DIN6-LUC* induction requires KIN10 kinase activity (K48) and T-loop phosphorylation (T175). D, dark; H, hypoxia; C, control DNA. Control, DCMU and hypoxia treatments were performed under light (50 $\mu\text{mol m}^{-2}\text{s}^{-1}$). Error bars, s.d. (n = 3). Protein expression was confirmed by western blot analysis.

¹Department of Genetics, Harvard Medical School, and Department of Molecular Biology, Massachusetts General Hospital, Boston Massachusetts 02114, USA. ²Department of Molecular Microbiology, VIB, B-3001 Leuven-Heverlee, Flanders, Belgium. ³Laboratory of Molecular Cell Biology, Institute of Botany and Microbiology, K.U.Leuven, Kasteelpark Arenberg 31, B-3001 Leuven-Heverlee, Flanders, Belgium.

*These authors contributed equally to this work.

model system using a sensitive reporter, generated by fusing the putative promoter of *Arabidopsis* *DIN6* (encoding the glutamine-dependent asparagine synthetase, *ASN1*) to the luciferase (*LUC*) gene (Methods Summary). In transfected mesophyll protoplasts, *DIN6-LUC* was activated by darkness, DCMU, hypoxia/submergence and other stresses within 3–6 h (Fig. 1d, and J.S., unpublished), in a similar way to the endogenous *DIN6* gene^{8,11–13} (Fig. 1a–c; and Supplementary Fig. 2a). This activation was repressed by sucrose or glucose at physiological concentrations as low as 5 mM (Supplementary Fig. 2b). Interestingly, endogenous *DIN6* activation by diverse signals was abolished by the protein kinase inhibitor K252a (Supplementary Fig. 2c), suggesting the requirement of protein kinases in the integration of stress and sugar signals.

We first investigated the involvement of members of the Snf1-related kinase (SnRK) gene families³ (Supplementary Fig. 3a), implicated in metabolic regulation owing to their sequence homology to the yeast Snf1 and mammalian AMPKs^{3,14,15}. Cell-based functional screens revealed the specific activation of *DIN6-LUC* by the two ubiquitously expressed members of the SnRK1 group, KIN10 and KIN11 (Fig. 1e, and Supplementary Fig. 3b, c). Representative SnRK2 and SnRK3 members lacked the same function (Fig. 1e) despite their established protein kinase activities in osmotic and salt stress responses (Methods Summary). Expression of KIN10 and KIN11 in protoplasts conferred significant kinase activity, which required the conserved ATP binding site (K48 and K49) and T175 (ref. 14; Supplementary Fig. 4, and Fig. 1f). However, unlike T172 phosphorylation in AMPK, T175 phosphorylation in KIN10 was not correlated with activation by dark, DCMU or hypoxia treatment (data not shown). Thus, *DIN6-LUC* served as a sensitive and quantitative transcription reporter to monitor endogenous KIN10/11 activity *in vivo*.

To identify critical DNA sequences involved in the stress and KIN10-mediated responses, we performed systematic mutagenesis of predicted *cis*-regulatory elements (Supplementary Methods) in the *DIN6* promoter (Supplementary Fig. 5, and Fig. 2a). Significantly, specific mutation of the G-box (CACGTG, G1) proximal to the TATA box abolished most of the *DIN6-LUC* activation by KIN10, hypoxia, darkness and DCMU (Fig. 2b–d). The results indicate that a common *cis*-element mediates convergence of diverse signals, most probably through KIN10.

To substantiate this finding further, we screened *Arabidopsis* bZIP transcription factors¹⁶ that have been characterized as G-box binding factors (GBFs), and found that GBF5/bZIP2 (At2g18160) specifically activated *DIN6-LUC* (Fig. 2e). Importantly, co-expression of KIN10 with GBF5 resulted in a dramatic and synergistic effect on *DIN6-LUC* activation. Both the GBF5 effect and its synergism with KIN10 were abolished by the specific *DIN6* promoter mutation in the G-box *g1* (Fig. 2f). Similar results were obtained with closely related bZIP S-group members expressed in mesophyll cells (bZIP11/ATB2, At4g34590; bZIP53, At3g62420; and related bZIP1, At5g49450; Supplementary Table 1 and Fig. 2g, h). Functional redundancy of the transcription factors was evident also from the lack of overt phenotypes in the available loss-of-function single *bzip* mutants (data not shown). Because the S- and C-group bZIPs have been shown to form functional heterodimers¹⁶, we also examined the activity of C-group bZIPs. Interestingly, one member of the C-group, bZIP63, showed little activity alone but exhibited moderate synergism with KIN10 through the G-box (Fig. 2h). These studies identified novel functions of specific GBFs/bZIPs and provide further evidence for convergent responses in stress signalling through KIN10 and KIN11.

To explore the extent of KIN10 transcriptional regulation and identify its early target genes, we scaled-up transient protoplast expression experiments, which could rule out secondary or long-term effects of metabolism and growth, and circumvent limitations caused by redundancy and embryonic lethality observed in mammals and plants^{15,17,18}. Gene expression profiles with or without KIN10

expression were compared using *Arabidopsis* whole-genome ATH1 GeneChips (GEO accession number GSE8257; Supplementary Methods). To filter candidate KIN10 target genes (at least twofold change with P value < 0.0004), we combined independent experimental validation using quantitative real-time reverse transcriptase PCR (qRT-PCR) with vigorous statistical analyses of GeneChip data from biological replicates, using parametric and non-parametric methods (see Supplementary Methods and Supplementary Fig. 6 for details). Guided by the experimentally validated *MYB75* transcription factor gene and 24 other marker genes, we were able to define 1,021 putative KIN10 target genes that exhibited reproducible activation or repression (Supplementary Tables 1–3).

To increase robustness and assess the physiological significance of the co-regulation of KIN10 target genes, we performed additional computational screens to identify seven highly correlated gene expression patterns from published data sets generated with the *Arabidopsis* ATH1 GeneChips^{11–13,19–22} (details in Supplementary

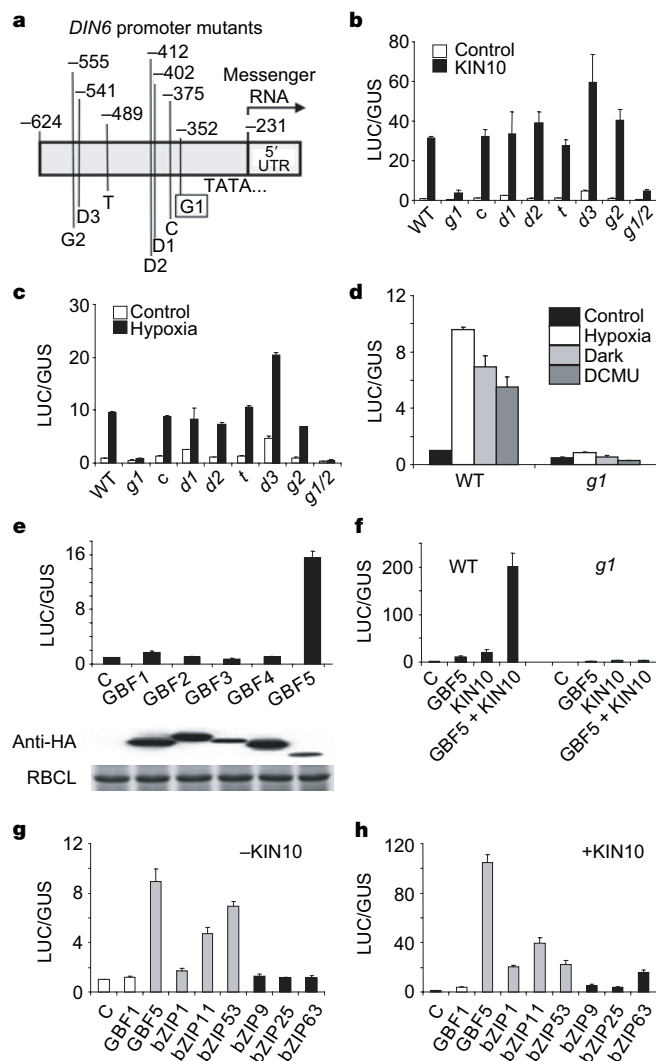


Figure 2 | Convergent transcriptional control through a G-box and specific GBFs. a–d, Mutational analysis of the *DIN6* promoter. G, G-box; T, TATCCA element; D, DOF-binding *cis*-element; C, C-box/ACGT/OSAMY3. Numbers are relative to ATG. The *g1* mutation prevents activation by KIN10 (b), hypoxia (c), dark and DCMU (d). e, *DIN6-LUC* is specifically induced by GBF5. f, KIN10 and GBF5 synergistically activate *DIN6-LUC* through the G1 box. g, Functional redundancy of S-group bZIPs (grey) in *DIN6-LUC* activation. h, Synergistic activation of *DIN6-LUC* by KIN10 and S-group (grey) and C-group (black; bZIP63) bZIPs. WT, wild-type *DIN6* promoter; C, control DNA. Control, DCMU, and hypoxia treatments were performed under light. Error bars, s.d. ($n = 3$).

Methods). Specifically, gene expression profiles generated under various sugar and energy starvation conditions^{11,20–22} revealed a striking positive correlation with KIN10 target genes (Pearson correlation coefficient 0.85 to 0.87, Supplementary Table 5). Importantly, KIN10 target genes also exhibited strong negative correlations (Pearson correlation coefficient -0.87 to -0.92 , Supplementary Table 5) with the gene expression profiles obtained from glucose- or sucrose-treated seedlings and differential CO₂-fixing adult leaves in intact plants^{12,13,19}.

A final filtering step was applied to remove genes with inconsistent expression patterns in any of the seven data sets. The stringent and multi-step filtering processes selected a reliable list of 278 genes co-activated by KIN10 and sugar starvation conditions, and co-repressed in sugar-treated seedlings or CO₂-fixing adult leaves (Fig. 3a, and Supplementary Table 4). A second list of 322 genes was also identified on the basis of their co-repression by KIN10 and sugar starvation conditions, but co-activation in sugar-treated seedlings or differential CO₂-fixing adult leaves (Fig. 3b, and Supplementary Table 4). As predicted by the *DIN* gene response (Fig. 1), hypoxia-treated protoplasts also displayed gene expression profiles similar to KIN10 overexpression on the basis of ATH1 GeneChip (GEO accession number GSE8248) and triplicated analyses of selected marker genes by qRT-PCR (Supplementary Fig. 7a, b). The correlation across the data sets (Supplementary Table 5) was remarkable considering the diversity of materials and experimental conditions used for the comparison and filtering (see Supplementary Methods). This suggests that KIN10 regulation is a cell-autonomous and ubiquitous event and highlights its physiological relevance.

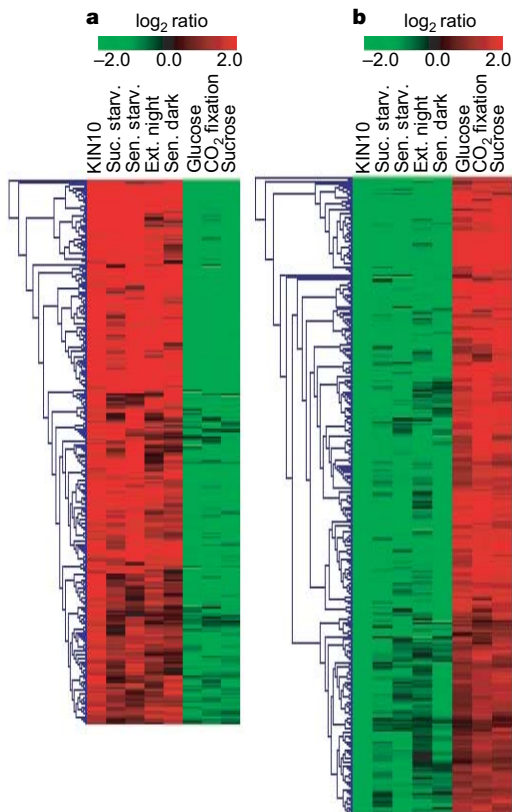


Figure 3 | Global gene expression regulation by KIN10. a, b, Transient *KIN10* expression in protoplasts results in the induction (a) and repression (b) of genes involved in a wide variety of cellular processes and metabolism (Supplementary Fig. 7c–e, and Supplementary Tables 3, 4). The KIN10-mediated gene expression profile is positively correlated with that regulated by sugar and carbon deprivation, and negatively correlated with that controlled by sugars (see text for details). Ext., extended; sen., senescence; starv., starvation; suc., sucrose.

Previous studies have identified specific SnRK1 target genes, one each in potato and wheat^{3,5}. The present work provides for the first time a complete overview of the surprisingly broad genome-wide transcript changes induced by these conserved protein kinases in a multicellular organism. The most prominent KIN10-activated (and sugar-repressed) genes represented a variety of major catabolic pathways, including cell wall, starch, sucrose, amino acid, lipid, and protein degradation that provide alternative sources of energy and metabolites (Supplementary Fig. 7c, and Supplementary Tables 3, 4). KIN10 also induced several *APG/ATG* (*AUTOPHAGY*) orthologues and plant-specific trehalose metabolism genes (*TPS8-11*), which potentially alter or sense the level of trehalose-6-P, a regulator of plant carbohydrate metabolism, growth and development^{23,24}. Conversely, a large set of genes involved in energy-consuming ribosome biogenesis (87 genes) and anabolism (Supplementary Fig. 7d, e) were co-ordinately repressed by KIN10 (Supplementary Tables 3, 4). Although many plant metabolic pathways have been well characterized at the biochemical level, their molecular regulatory mechanisms are still poorly understood. Thus, besides the well-known roles of SnRK1 in phosphorylating and modulating enzymes important for carbon and nitrogen metabolism^{3,14,25,26}, the present work identifies KIN10 and KIN11 as global regulators of gene expression involved in primary and secondary metabolism and protein synthesis^{11–13,19–22,27}. The results also reveal central and previously unrecognized regulatory roles of the plant SnRK1 (and possibly also mammalian AMPK) in controlling a large number of genes encoding transcription factors, chromatin remodelling factors, and a plethora of signal transduction components (Supplementary Fig. 7c, e, and Supplementary Tables 3, 4).

Significantly, many KIN10 marker genes induced by multiple stresses are primary glucose repressible genes insensitive to cycloheximide¹² and direct targets of GBF5 (Supplementary Fig. 7f). These genes are not induced by the inactive KIN10 K48M or T175A mutant (data not shown), pointing to a requirement of KIN10 protein kinase activity for this global gene expression response. Our results suggest that KIN10/11 initiate multiple transcription cascades in response to sugar or energy depletion in darkness and stress conditions. Coordinated transcription activation of direct target genes is at least in part exerted through GBF5 and related bZIP transcription factors. Future analyses will aim at elucidating the precise molecular link between the protein kinases and transcription factors.

To study the long-term effects of KIN10 activity at the whole-plant level, we generated *Arabidopsis* transgenic plants overexpressing *KIN10* (*O1* and *O2*) or with reduced *KIN10* expression using RNA interference (RNAi; *10-1* and *10-2*) (Supplementary Fig. 8a). The *KIN10* overexpression seedlings displayed some advantage in primary root growth and development under low light with limited energy supply (Supplementary Fig. 8b, e). With exogenous sucrose, *KIN10* overexpression plants showed reduced growth in shoots and roots, possibly owing to KIN10 repression of biosynthetic activities (Supplementary Fig. 8c–e). In contrast, the *KIN10* silenced lines were able to use exogenously supplied sucrose (Supplementary Fig. 8c–e) and glucose (data not shown) more efficiently and exhibited enhanced shoot and root growth. Growth on 3% sucrose also increased anthocyanin accumulation in wild-type, *10-1* and *10-2* plants, but not in the *KIN10* overexpression lines (Supplementary Fig. 8f). Consistently, *KIN10* overexpression repressed the expression of *MYB75/PAP1* (At1g56650) (Supplementary Table 3), a key transcription factor for anthocyanin biosynthesis (Supplementary Methods).

A role of KIN10 in the starvation response was most evident after transferring seedlings to glucose-free liquid medium under a low light intensity that limits photosynthesis. Whereas wild-type seedlings underwent rapid senescence on nutrient deprivation, *KIN10* overexpression promoted plant survival (Fig. 4a). When grown in soil, *KIN10* overexpression altered inflorescence architecture (Fig. 4b, c) and delayed flowering and onset of senescence under long-day

conditions (20 h light/4 h dark) (Fig. 4c). This is reminiscent of life-span extension by calorie restriction in animals and provides evidence for a new role of KIN10 in determining plant shape and developmental transition timing and linking this to metabolism and environmental cues. Soil-grown *10-1* and *10-2* lines did not show an obvious phenotype, probably owing to functional redundancy of KIN11.

To circumvent the experimental limitation of obtaining double loss-of-function mutants^{3,17,18}, we generated *kin11* single- and *kin10 kin11* double-mutant plants, using virus-induced gene silencing (VIGS)²⁸ of *KIN11* in wild-type and *10-1* or *10-2* transgenic seedlings. Reduction of *KIN* transcripts was confirmed by RT-PCR and immunoblotting (using KIN10 and P-AMPK antibodies; Supplementary Fig. 9a) before extensive phenotypic and molecular studies. Three weeks after infiltration, double mutants *d-1* and *d-2* showed a surprisingly dramatic growth defect with small leaves and short petioles under 13 h light/11 h dark (Fig. 4d, and Supplementary Fig. 9b) or constant illumination conditions (data not shown). A strong accumulation of anthocyanins, curling of new leaves (leaves 11–12) and symptoms of early senescence were visible (Fig. 4d). The impact on growth and senescence in *d-1* and *d-2* lines was most striking five weeks after infiltration, when the transition to the reproductive phase occurred in wild-type plants (Fig. 4e). The most severely silenced plants senesced before flowering (Fig. 4e), whereas those with milder silencing bolted but failed to produce viable primary inflorescences and axillary floral meristems (Fig. 4f). Unlike the *snf1a snf1b* double mutant in moss²⁹, the growth phenotypes could neither be rescued by continuous light irradiance nor by supplementation with 1% sucrose (data not shown). This argues against the growth defects being merely due to impaired catabolism, and supports a more fundamental and unexpected role of

KIN10/KIN11 in normal vegetative and reproductive growth and development in flowering plants.

To establish a definitive molecular and quantitative link between KIN10/11 action and the ability to mount transcription activation in response to stresses and energy deprivation, we examined the response to hypoxia, dark or DCMU in mesophyll cells and intact leaves of wild-type, single- and double-mutant plants. All KIN10 marker genes tested could no longer be activated by any of these stresses in the *d-1* and *d-2* double mutants (Fig. 4g, h; Supplementary Fig. 9c, d, and Supplementary Table 6). Consistent with a role of KIN10/11 in promoting catabolic processes, leaf starch—as a major carbon source in the absence of photosynthesis—remained high at the end of night in the *d-1* and *d-2* double mutants (Fig. 4i). This suggests that KIN10/11 may have a previously unrecognized regulatory role in starch mobilization at night³⁰. Alternatively, starch accumulation may reflect a reduced energy demand for growth. In the future, it will be interesting and informative to extend the analysis of gene expression reprogramming to changes in enzyme activities and metabolite homeostasis in response to environmental cues associated with KIN10/KIN11 regulation.

Our studies provide molecular, biochemical, genetic and genomic evidence for the essential functions of KIN10/KIN11 in plant protection and survival under stress, darkness and sugar deprivation conditions. Surprising roles of KIN10/KIN11 in vegetative and reproductive growth and developmental transition under normal conditions are uncovered (Supplementary Fig. 1). Their roles as energy sensors and integrators, orchestrating global transcription, may also be found in mammals and thus our findings in plants may contribute to the understanding of AMPK functions in relation to diabetes, cancer, obesity and longevity. Further dissection of the components and molecular mechanisms of the KIN10/KIN11

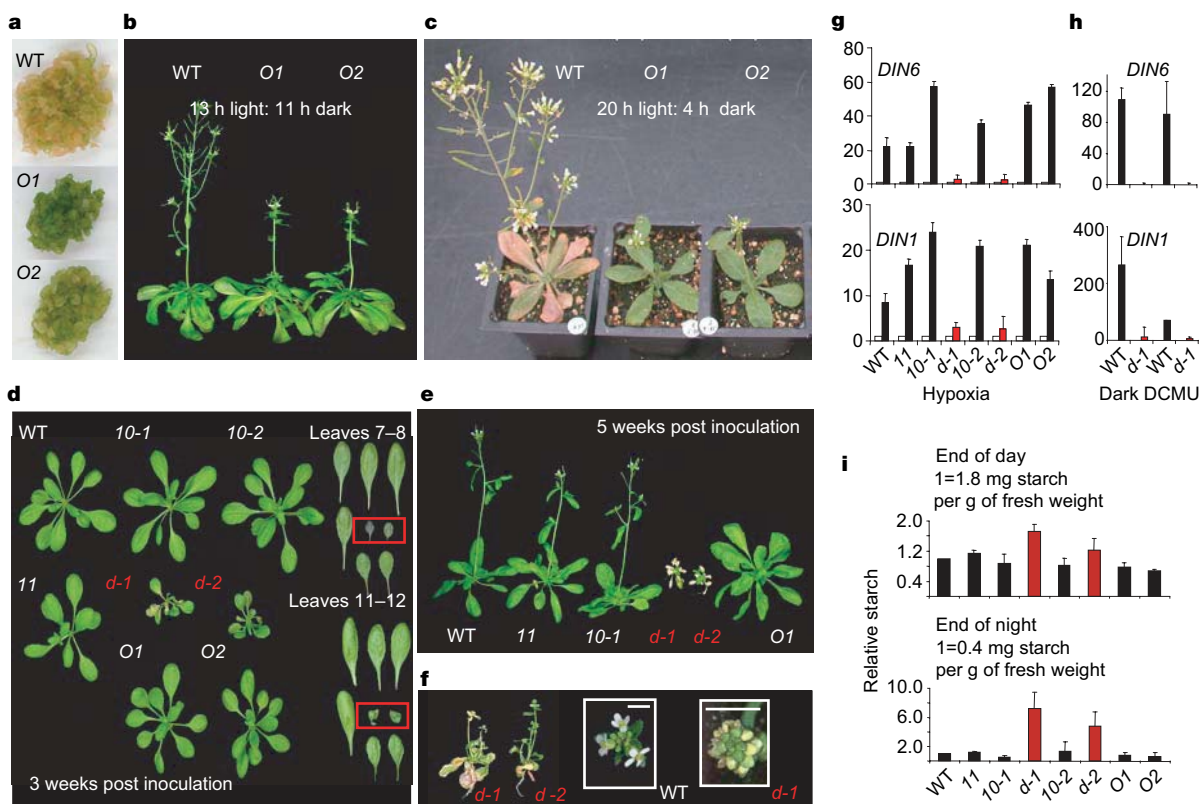


Figure 4 | Role of KIN10 in plant development, stress responses and starch mobilization at night. **a–c**, *KIN10* overexpression (*O1*, *O2*) prevents nutrient-deprivation-induced senescence (**a**), alters inflorescence development (**b**, **c**), and delays long-day-triggered senescence (**c**). **d–f**, *kin10 kin11* VIGS double mutant (*d-1*, *d-2*) plants show growth arrest (**d**) and premature senescence that precludes flowering (**e**), or bolting without

axillary floral meristems or viable inflorescences (inset) (**f**). The KIN10 target gene response to hypoxia (**g**, mesophyll cells) and dark or DCMU (**h**, leaves) is abolished in the double mutants (red). **i**, The double mutants are impaired in starch mobilization. *10-1/10-2*, *kin10* RNAi lines; *11*, *kin11* VIGS plants. Error bars, s.d. (**g**, **i**, $n = 3$; **h**, $n = 2$).

signalling cascades will provide valuable information on the metabolic control of plant growth and development, which may enable a more targeted genetic modification of plant development, architecture, carbon allocation, and stress resistance—all major determinants of crop yield and renewable energy production.

METHODS SUMMARY

Primers. All primers used are listed in Supplementary Table 7.

Effector and reporter constructs. *KIN10*, *KIN11*, *ASK1*, *ASK2* and the full-length and truncated *SOS2* (*ASOS2*, encoding amino acids 1–308) were fused to the haemagglutinin (HA) tag and cloned between a 35S-derived promoter and *NOS* terminator. The 624-bp promoter/5'-UTR sequence of *DIN6* was fused to the *LUC* reporter gene to generate *DIN6-LUC*.

Protoplast transient expression assay. Protoplast assays were performed using *UBQ10-GUS* as a transfection control. Protoplasts ($1-4 \times 10^4$) were incubated for 6 h in 1 ml of mannitol buffer in 6-well plates, or submerged in 1 ml of buffer in a 1.5 ml microfuge tube for hypoxia treatment. Protein expression was analysed using *KIN10*-specific rabbit antibody generated against a glutathione S-transferase (GST)-fused *KIN10* polypeptide (amino acids 335–388), human anti-P-AMPK (New England Biolabs), and a monoclonal anti-HA antibody (Roche). For dark treatment, plates were covered with aluminium foil. DCMU was added at 20 μ M. For global gene expression analyses, transfection experiments were scaled up 50-fold. For details on GeneChip experiments, data processing and analysis, see Supplementary Information.

Protein kinase assays. These were performed using immunoprecipitated HA-tagged kinases and SPS peptide (RDHMPRIRSEMQUIWSED) as a substrate.

Transgenics. To generate *KIN10* overexpression lines, the coding region was cloned in a pCB302-derived minibinary expression vector. For *KIN10RNAi*, the last 238 bp of the coding region (primers: 5'-cgggatccagcagcgcagatggtatg-3', 5'-aaggctcatgcatggtcagaggactcggagctgag-3') were cloned in both orientations, separated by an intron.

Virus-induced gene silencing (VIGS). *KIN11* VIGS was performed as described²⁸ using a gene-specific 503-bp *KIN11* fragment (–103 to +400, primers: 5'-ggaattcgttctgtatattctcgtc-3', 5'-cgggatccagctactctacaccagatattat-3') and repeated six times with consistent results.

Full Methods and any associated references are available in the online version of the paper at www.nature.com/nature.

Received 11 April; accepted 2 July 2007.

Published online 1 August 2007.

1. Yamaguchi-Shinozaki, K. & Shinozaki, K. Transcriptional regulatory networks in cellular responses and tolerance to dehydration and cold stresses. *Annu. Rev. Plant Biol.* **57**, 781–803 (2006).
2. Hasegawa, P. M., Bressan, R. A., Zhu, J.-K. & Bohnert, H. J. Plant cellular and molecular responses to high salinity. *Annu. Rev. Plant Physiol. Plant Mol. Biol.* **57**, 463–499 (2000).
3. Halford, N. G. *et al.* Metabolic signalling and carbon partitioning: role of Snf1-related (SnRK1) protein kinase. *J. Exp. Bot.* **54**, 467–475 (2003).
4. Bhalerao, R. P. *et al.* Regulatory interaction of PRL1 WD protein with *Arabidopsis* SNF1-like protein kinases. *Proc. Natl Acad. Sci. USA* **96**, 5322–5327 (1999).
5. Purcell, P. C., Smith, A. M. & Halford, N. G. Antisense expression of a sucrose non-fermenting-1-related protein kinase sequence in potato results in decreased expression of sucrose synthase in tubers and loss of sucrose-inducibility of sucrose synthase transcripts in leaves. *Plant J.* **14**, 195–202 (1998).
6. Tiessen, A. *et al.* Evidence that SNF1-related kinase and hexokinase are involved in separate sugar-signalling pathways modulating post-translational redox activation of ADP-glucose pyrophosphorylase in potato tubers. *Plant J.* **35**, 490–500 (2003).
7. Zimmermann, P., Hirsch-Hoffmann, M., Hennig, L. & Gruissem, W. GENEVESTIGATOR. *Arabidopsis* microarray database and analysis toolbox. *Plant Physiol.* **136**, 2621–2632 (2004).
8. Fujiki, Y. *et al.* Dark-inducible genes from *Arabidopsis thaliana* are associated with leaf senescence and repressed by sugars. *Physiol. Plant.* **111**, 345–352 (2001).
9. Moore, B. *et al.* Role of the *Arabidopsis* glucose sensor HXK1 in nutrient, light, and hormonal signaling. *Science* **300**, 332–336 (2003).
10. Rolland, F., Baena-González, E. & Sheen, J. Sugar sensing and signaling in plants: conserved and novel Mechanisms. *Annu. Rev. Plant Biol.* **57**, 675–709 (2006).
11. Lin, J. F. & Wu, S. H. Molecular events in senescing *Arabidopsis* leaves. *Plant J.* **39**, 612–628 (2004).
12. Price, J., Laxmi, A., St Martin, S. K. & Jang, J. C. Global transcription profiling reveals multiple sugar signal transduction mechanisms in *Arabidopsis*. *Plant Cell* **16**, 2128–2150 (2004).
13. Palenchar, P. M., Kouranov, A., Lejay, L. V. & Coruzzi, G. M. Genome-wide patterns of carbon and nitrogen regulation of gene expression validate the

combined carbon and nitrogen (CN)-signaling hypothesis in plants. *Genome Biol.* **5**, R91 (2004).

14. Hardie, D. G., Carling, D. & Carlson, M. The AMP-activated/SNF1 protein kinase subfamily: metabolic sensors of the eukaryotic cell? *Annu. Rev. Biochem.* **67**, 821–855 (1998).
15. Kahn, B. B., Alquier, T., Carling, D. & Hardie, D. G. AMP-activated protein kinase: ancient energy gauge provides clues to modern understanding of metabolism. *Cell Metab.* **1**, 15–25 (2005).
16. Jakoby, M. *et al.* bZIP transcription factors in *Arabidopsis*. *Trends Plant Sci.* **7**, 106–111 (2002).
17. Zhang, Y. *et al.* Expression of antisense SnRK1 protein kinase sequence causes abnormal pollen development and male sterility in transgenic barley. *Plant J.* **28**, 431–441 (2001).
18. Radchuk, R., Radchuk, V., Weschke, W., Borisjuk, L. & Weber, H. Repressing the expression of the *SUCROSE NONFERMENTING-1-RELATED PROTEIN KINASE* gene in pea embryo causes pleiotropic defects of maturation similar to an abscisic acid-insensitive phenotype. *Plant Physiol.* **140**, 263–278 (2006).
19. Bläsing, O. E. *et al.* Sugars and circadian regulation make major contributions to the global regulation of diurnal gene expression in *Arabidopsis*. *Plant Cell* **17**, 3257–3281 (2005).
20. Buchanan-Wollaston, V. *et al.* Comparative transcriptome analysis reveals significant differences in gene expression and signalling pathways between developmental and dark/starvation-induced senescence in *Arabidopsis*. *Plant J.* **42**, 567–585 (2005).
21. Contento, A. L., Kim, S. J. & Bassham, D. C. Transcriptome profiling of the response of *Arabidopsis* suspension culture cells to Suc starvation. *Plant Physiol.* **135**, 2330–2347 (2004).
22. Thimm, O. *et al.* MAPMAN: a user-driven tool to display genomics data sets onto diagrams of metabolic pathways and other biological processes. *Plant J.* **37**, 914–939 (2004).
23. Schlupepman, H., Pellny, T., van Dijken, A., Smeekens, S. & Paul, M. Trehalose 6-phosphate is indispensable for carbohydrate utilization and growth in *Arabidopsis thaliana*. *Proc. Natl Acad. Sci. USA* **100**, 6849–6854 (2003).
24. Gomez, L. D., Baud, S., Gilday, A., Li, Y. & Graham, I. A. Delayed embryo development in the *ARABIDOPSIS* *TREHALOSE-6-PHOSPHATE SYNTHASE 1* mutant is associated with altered cell wall structure, decreased cell division and starch accumulation. *Plant J.* **46**, 69–84 (2006).
25. Sugden, C., Donaghy, P. G., Halford, N. G. & Hardie, D. G. Two SNF1-related protein kinases from spinach leaf phosphorylate and inactivate 3-hydroxy-3-methylglutaryl-coenzyme A reductase, nitrate reductase, and sucrose phosphate synthase *in vitro*. *Plant Physiol.* **120**, 257–274 (1999).
26. Kaiser, W. M. & Huber, S. C. Post-translational regulation of nitrate reductase: Mechanism, physiological relevance and environmental triggers. *J. Exp. Bot.* **52**, 1981–1989 (2001).
27. Li, Y. *et al.* Establishing glucose- and ABA-regulated transcription networks in *Arabidopsis* by microarray analysis and promoter classification using a Relevance Vector Machine. *Genome Res.* **16**, 414–427 (2006).
28. Burch-Smith, T. M., Schiff, M., Liu, Y. & Dinesh-Kumar, S. P. Efficient virus induced gene silencing in *Arabidopsis thaliana*. *Plant Physiol.* **142**, 21–27 (2006).
29. Thelander, M., Olsson, T. & Ronne, H. Snf1-related protein kinase 1 is needed for growth in a normal day–night light cycle. *EMBO J.* **23**, 1900–1910 (2004).
30. Smith, A. M., Zeeman, S. C. & Smith, S. M. Starch degradation. *Annu. Rev. Plant Biol.* **56**, 73–98 (2005).

Supplementary Information is linked to the online version of the paper at www.nature.com/nature. A model for *KIN10/11* function is available in Supplementary Information (Supplementary Fig. 1).

Acknowledgements We thank S. P. Dinesh-Kumar for generously sharing the TRV-based vectors and the VIGS protocol for *Arabidopsis* plants before publication, O. Thimm and M. Stitt for the MAPMAN program and the original functional classification files, J.C. Jang, S. Wu and D.C. Bassham for sharing the original GeneChip data, B. Wittner for consultation on the RankProd analysis, Q. Hall for the pQH29 RNAi vector, L. Zhou for the *DIN6-LUC* construct, L. Shan and P. He for the VIGS GFP control vector and the infiltration procedure, J. Bush for plant management, K. Chu for data analysis, and the Sheen laboratory members for stimulating discussions. The work was supported by grants from the National Science Foundation and National Institute of Health to J.S.F.R. was supported by a return grant from the Belgian Office for Scientific, Technical and Cultural Affairs and fellowships from the Belgian American Educational Foundation and the Research Foundation–Flanders (FWO–Vlaanderen).

Author Information All microarray data are available at the Gene Expression Array Omnibus website (<http://www.ncbi.nlm.nih.gov/geo/>) under accession numbers GSE8248 and GSE8257. Reprints and permissions information is available at www.nature.com/reprints. The authors declare no competing financial interests. Correspondence should be addressed to F.R. (filip.rolland@bio.kuleuven.be) and requests for materials should be addressed to F.R. and E.B.-G. (baena@molbio.mgh.harvard.edu).

METHODS

Phylogenetic tree. For generation of the phylogenetic tree (Supplementary Fig. 3a), protein sequences were aligned with ClustalW, using the SDSC Workbench (workbench.sdsc.edu).

Effector and reporter constructs. Effector constructs—*KIN10* (SnRK1.1; At3g01090), *KIN11* (SnRK1.2; At3g29160), and *SOS2* (SnRK3.11; At5g35410)—were amplified from leaf complementary DNA, fused to the HA tag, and cloned between a 35S-derived promoter and *NOS* terminator^{31–33}. The *ASK1* (SnRK2.4; At1g10940) and *ASK2* (SnRK2.1; At5g08590), and the constitutively active version of *SOS2* (Δ SOS2, amino acids 1–308) were as described^{31,34,35}. Reporter construct: The 624-bp promoter/5'-UTR sequence of *DIN6* (At3g47340) was fused to the *LUC* reporter gene to generate *DIN6-LUC* as described^{32,33,36}. The kinase (K48M, K49M, T175A) and *DIN6* promoter mutants were generated by site-directed mutagenesis, as described³³.

Protoplast transient expression assay and treatments. Protoplast transient expression assays were carried out as described^{32,33,37}, using 35S-*GUS* or *UBQ10-GUS* reporter gene fusions as transfection controls^{32,33}. Data were generated from at least three independent experiments with consistent results. Protoplasts ($1-4 \times 10^4$) were incubated for 6 h in 1 ml of mannitol buffer in 6-well tissue culture plates (1 mm depth, excluding hypoxia effects)^{32,33,37} or submerged in 1 ml of mannitol buffer in a 1.5 ml microfuge tube (25-mm depth) for hypoxia treatment. Establishment of the hypoxic condition was confirmed by the induction of well-known hypoxia marker genes encoding ADH and PDC (refs. 38, 39) in qRT-PCR and microarray analyses (data not shown). These genes are induced under hypoxic and anoxic conditions, but not under other types of cellular energy stress. Unlike *DIN1* and *DIN6*, their induction cannot be repressed by sugar³⁹. For dark treatment, plates were covered with aluminium foil for 6 h. If not otherwise indicated, DCMU, glucose and sucrose, were added to final concentrations of 20 μ M, 25 mM and 50 mM, respectively.

RT-PCR analysis. The fifth and sixth leaves of 4-week-old plants, protoplasts and one-week-old seedlings were treated with darkness (leaves and protoplasts, 6 h; leaves of VIGS plants, 10 h; seedlings, 20 h), DCMU (leaves and seedlings, 100 μ M, 20 h; leaves of VIGS plants, 100 μ M, 10 h; protoplasts, 50 μ M, 6 h) or submerged in water (hypoxia treatment, leaves and seedlings, 20 h; protoplasts, 6 h) in the absence or presence of 3% sucrose, 25 mM glucose, or a protein kinase inhibitor K252a (2 μ M). RNA samples were isolated and analysed by RT-PCR for *DIN1* and *DIN6* expression using gene-specific primers (Supplementary Table 7). *UBQ4* was used as a control gene. Total RNA (1 μ g) was converted to single-stranded complementary DNA by reverse transcriptase (Invitrogen). Quantitative real time RT-PCR (qRT-PCR) was performed using PCR Master Mix SYBR Green (BioRad) in a BioRad iCycler (3 min 95 °C, 40 cycles at 10 s 95 °C, 45 s at 59 °C, and 1 min 95 °C, 1 min 55 °C). In the protoplast assays, marker gene expression was normalized to *CIPK23* (At1g30270) expression, chosen on the basis of its steady levels in the *KIN10* and hypoxia GeneChip experiments (Supplementary Table 1). In the leaf assays, marker gene expression was normalized to *TUB4* (At5g44340).

Protein kinase assays. Kinase assays were performed as described⁴⁰ using HA-tagged kinases immunoprecipitated from protoplasts and the SPS peptide (RDHMPRIKSEMQUIWSED) as a specific substrate⁴¹. Kinase reaction mixes were spotted onto Whatman P81 phosphocellulose paper squares and the reactions were terminated by immersion in 75 mM phosphoric acid. Squares were washed twice, airdried and incorporated radioactivity was measured by liquid scintillation counting.

Antibodies and protein expression analyses. To generate the *KIN10*-specific antibody, a GST-fused *KIN10* polypeptide (amino acids 335–388) was produced in *E. coli* using a pGEX-4T-1 vector and GST was removed before rabbit injection. The antibody was affinity purified using a SulfoLink matrix (Pierce). Phospho-*KIN10* and phospho-*KIN11* were detected using a commercial antibody against the human phospho-AMPK α subunit (P-AMPK, New England Biolabs). HA-tagged proteins were detected by an anti-HA monoclonal antibody (Roche) using standard techniques³³.

Transgenics. To generate transgenic *KIN10* overexpression lines, the coding region was cloned into an expression vector derived from the pCB302 minibinary vector³³. For generating the *kin10* RNAi lines, the last 238 bp of the coding region was cloned into pQH29 in both orientations separated by an intron (Q. Hall, unpublished information) and sub-cloned into the pCB302-derived expression vector³³. Multiple transgenic lines were generated by standard protocols³³, screened by RT-PCR and analysed for consistent phenotypes.

Loss-of-function transgenics. No T-DNA insertion, enhancer or gene trap knockout lines with significantly reduced *KIN10* or *KIN11* expression could

be obtained (data not shown). We also attempted to generate *kin11* single and *kin10 kin11* double mutants using the same RNAi strategy. However, despite multiple efforts and extensive transgenic screens, we were not able to recover transgenic lines, possibly because of embryonic lethality^{3,15}. Studies in barley pollen¹⁷ and pea seed¹⁸ have shown that antisense expression of *SnRK1* causes male sterility and embryo maturation defects, consistent with our inability to obtain transgenic *Arabidopsis* lines with deficiency in both *KIN10* and *KIN11*.

Virus-induced gene silencing (VIGS). VIGS was performed as described using *Arabidopsis* wild-type, *KIN10*-overexpressing, and *kin10* RNAi seedlings^{28,42–44}. The control VIGS construct was generated using a 596-bp *GFP* fragment and the *KIN11* VIGS construct, using a gene-specific 503-bp fragment (103 bp of the 5' UTR and the first 400 bp of the *KIN11* coding region). The mutant plants were identified by RT-PCR and the VIGS experiments were repeated six times with consistent results.

Plant growth and phenotype assays. Plants were grown in soil under standard 13 h light/11 h dark or 20 h light/4 h dark (long-day) conditions. For the various phenotype assays, seedlings were grown under constant light (80 μ E) in liquid medium: (1) 0.5 \times MS, 0.5% sucrose, 60 r.p.m. for 7 days for dark, DCMU, and hypoxia treatments; (2) MS, 2% glucose, 60 r.p.m. for 7 days and transferred to glucose-free medium for 2 weeks, for nutrient starvation assays; (3) MS, 3% sucrose, 60 r.p.m. for 7 days for spectrophotometric anthocyanin quantification (OD_{530}). To test the effect of sugar availability on growth, seedlings were grown for 11 d vertically on agar plates (0.1 \times MS \pm sucrose) under 16 h light/8 h dark conditions.

Starch quantification. Starch was extracted from 0.2–0.3 g (fresh weight) of leaf material and quantified using a starch assay kit (Sigma)⁴⁵.

URLs. Geneinvestigator is available at <http://www.geneinvestigator.ethz.ch/>; MAPMAN, at <http://gabi.rzpd.de/projects/MapMan/>; NASC International Affymetrix Service at <http://affymetrix.arabidopsis.info/>; and TIGR MeV at <http://www.tmg4.org/mev.html>. Gene annotation information is available on the Sheen lab website at http://genetics.mgh.harvard.edu/sheenweb/search_affy.html.

31. Kovtun, Y., Chiu, W.-L., Zeng, W. & Sheen, J. Suppression of auxin signal transduction by a MAPK cascade in higher plants. *Nature* **395**, 716–720 (1998).
32. Kovtun, Y., Chiu, W.-L., Tena, G. & Sheen, J. Functional analysis of oxidative stress-activated MAPK cascade in plants. *Proc. Natl Acad. Sci. USA* **97**, 2940–2945 (2000).
33. Hwang, I. & Sheen, J. Two-component circuitry in *Arabidopsis* cytokinin signal transduction. *Nature* **413**, 383–389 (2001).
34. Guo, Y., Halfter, U., Ishitani, M. & Zhu, J. K. Molecular characterization of functional domains in the protein kinase *SOS2* that is required for plant salt tolerance. *Plant Cell* **13**, 1383–1400 (2001).
35. Boudsocq, M., Barbier-Brygoo, H. & Lauriere, C. Identification of nine sucrose nonfermenting 1-related protein kinases 2 activated by hyperosmotic and saline stresses in *Arabidopsis thaliana*. *J. Biol. Chem.* **279**, 41758–41766 (2004).
36. Lam, H. M., Peng, S. S. & Coruzzi, G. M. Metabolic regulation of the gene encoding glutamine-dependent asparagine synthetase in *Arabidopsis thaliana*. *Plant Physiol.* **106**, 1347–1357 (1994).
37. Sheen, J. Signal transduction in maize and *Arabidopsis* mesophyll protoplasts. *Plant Physiol.* **127**, 1466–1475 (2001).
38. Gonzali, S. et al. The use of microarrays to study the anaerobic response in *Arabidopsis*. *Ann. Bot. (Lond.)* **96**, 661–668 (2005).
39. Loreti, E., Poggi, A., Novi, G., Alpi, A. & Perata, P. A genome-wide analysis of the effects of sucrose on gene expression in *Arabidopsis* seedlings under anoxia. *Plant Physiol.* **137**, 1130–1138 (2005).
40. Cheng, S.-H., Sheen, J., Gerrish, C. & Bolwell, G. P. Molecular identification of phenylalanine ammonia-lyase as a substrate of a specific constitutively active *Arabidopsis* CDPK expressed in maize protoplasts. *FEBS Lett.* **503**, 185–188 (2001).
41. Huang, J. Z. & Huber, S. C. Phosphorylation of synthetic peptides by a CDPK and plant SNF1-related protein kinase. Influence of proline and basic amino acid residues at selected positions. *Plant Cell Physiol.* **42**, 1079–1087 (2001).
42. Liu, Y., Schiff, M. & Dinesh-Kumar, S. P. Virus-induced gene silencing in tomato. *Plant J.* **31**, 777–786 (2002).
43. Ryu, C. M. A. n. a. n. d. A., Kang, L. & Mysore, K. S. Agrodrench: a novel and effective agroinoculation method for virus-induced gene silencing in roots and diverse Solanaceous species. *Plant J.* **40**, 322–331 (2004).
44. Burch-Smith, T. M., Anderson, J. C., Martin, G. B. & Dinesh-Kumar, S. P. Applications and advantages of virus-induced gene silencing for gene function studies in plants. *Plant J.* **39**, 734–746 (2004).
45. Kötting, O. et al. Identification of a novel enzyme required for starch metabolism in *Arabidopsis* leaves. The phosphoglucan, water dikinase. *Plant Physiol.* **137**, 242–252 (2005).